

Assessment of Earth Remote Sensing Microsatellite Power Subsystem Capability during Detumbling and Nominal Modes

M. Zahran^{†*}, M. Okasha^{*} and Galina A. Ivanova^{**}

[†]Electronics Research Institute, NRC Bldg., El-Tahrir St., Dokki, 12311-Giza, Egypt

^{*}National Authority for Remote Sensing and Space Science, Cairo Egypt

^{**}Yuzhnoye State Design Office, 3, Kryvorozhskaya st., Dnepropetrovsk, Ukraine

ABSTRACT

The Electric Power Subsystem (EPS) is one of the most critical systems on any satellite because nearly every subsystem requires power. This makes the choice of power systems the most important task facing satellite designers. The main purpose of the Satellite EPS is to provide continuous, regulated and conditioned power to all the satellite subsystems. It has to withstand radiation, thermal cycling and vacuums in hostile space environments, as well as subsystem degradation over time^[1]. The EPS power characteristics are determined by both the parameters of the system itself and by the satellite orbit^[2]. After satellite separation from the launch vehicle (LV) to its orbit, in almost all situations, the satellite subsystems (attitude determination and control, communication and onboard computer and data handling (OBC&DH)), take their needed power from a storage battery (SB) and solar arrays (SA) besides the consumed power in the EPS management device. At this point (separation point, detumbling mode), the satellite's angular motion is high and the orientation of the solar arrays, with respect to the Sun, will change in a non-uniform way, so the amount of power generated by the solar arrays will be affected.

The objective of this research is to select satellite EPS component types, to estimate solar array illumination parameters and to determine the efficiency of solar arrays during both detumbling and normal operation modes.

Keywords: Earth Remote Sensing, EPS System Design, GaAs, NiCd, Low Earth Orbit(LEO), Orbit and Attitude Dynamics, Detumbling mode, Direct Energy Transfer(DET), Orbit Illumination, Energy Management and Control

1. Introduction

During mission analysis, it is important to determine the total required power for nominal and off-nominal

operations of satellite subsystems during different modes of operation, which in turn will play a great role in the selection of a suitable battery, their capacity and sizing of solar arrays.

Most satellites use storage batteries (NiCd, usually NiH₂) to store excess energy generated by the solar arrays during periods of exposure to the Sun. During an eclipse, the batteries are used to provide power for the satellite subsystems. The batteries are recharged when the satellite exits the eclipse^[3]. The data of interest to EPS designers

Manuscript received Nov. 4, 2004; revised Oct. 16, 2005

[†]Corresponding Author: Zahran@eri.sci.eg

Tel: +202-331-0512, Fax:+202-335-1631, ERI, NARSS

^{*}National Authority for Remote Sensing and Space Science

^{**}Yuzhnoye State Design Office

are orbit altitude, orbit inclination and the local time of ascending nodes, both average and peak power budgets and lifetime. These parameters have an influence on the following:

- The power generated by SA,
- The temperature of the effective area of the SA,
- The depth and the duration of the temperature cycles,
- The level of damage to the satellite equipment due to the Earth radiation,
- The number and depth of the charge and discharge cycles of the SB, and
- Energy balance during the mission life.

The size of the microsatellite EPS components depends strongly on the orbital parameters and the power budget of the satellite onboard equipment that is represented by the load profile, that is, a graphical representation of the power requirements of the satellite loads with time. The satellite's orbital parameters that affect the EPS operation are simulated during the lifetime to estimate the illumination coefficient of the EPS solar array, taking into consideration the space environment and orbital perturbation. The most critical period of the satellite EPS operation starts from the satellite separation from the launch vehicles up until it reaches the steady state (oriented) operation. In this period, the satellite onboard equipment depends strongly on the storage battery since the output power from the solar array is much lower than nominal.

When the satellite separates from the launch vehicle, it separates with high angular velocities. So, its attitude changes quickly and a control algorithm is used to suppress these angular velocities and to construct an attitude. During this stage (detumbling mode), the attitude of the solar arrays, relative to the Sun, will also change rapidly and the efficiency of charging and discharging the chemical battery will be affected much more during that stage.

The power generated by the solar arrays mainly depends on the angle between the direction to the Sun and the normal angle to its surface. To calculate this angle, a mathematical model will be constructed to simulate the satellite in its orbit to determine the solar arrays' attitude with respect to the Sun. To do that, a mathematical model of satellite orbital/attitude motion besides the Sun's

motion will be developed, also a control algorithm will be selected to suppress the satellite's angular motion and counteract the environmental disturbances.

2. Basics of EPS Selection

The optimum choice of the EPS components is not usually an easy task for the satellite designers due to the closed interaction between the EPS and the directives of the satellite's mission. The designers must be aware of the various power subsystems available for use on the satellite. Figure 1 shows the most suitable power sources onboard the satellite, depending on the information about the onboard equipment (OBE) average power requirements and satellite design lifetime. The satellite under this study is an Earth remote sensing microsatellite, in the Sun-synchronous orbit with a planned five year lifetime. Applying such information to the EPS selection chart we can conclude that the most suitable primary source for the proposed satellite is the photovoltaic (solar arrays).

2.1 Solar Array Type Estimation

Several proven solar array technologies compete for the satellite market. These are single crystal Si solar cells, thin crystalline Si cells, GaAs solar cells, InP solar cells, and the cascaded solar cells. Table 1 summarizes the important characteristics of each technology.

Table 1 solar cell technologies for space applications

	Crystal-line. Si	Thin Si	GaAs	InP	Cascaded
Cell eff. %	22	17	23	19	30
Array eff. %	10-15	8	19-21		17
Specific mass	0.42		0.36		
Lifetime and reliability	Med	Low	High	High	High
Radiation tolerance *:					
1 MeV electrons	10		33	155	
10 MeV protons	2		6	89	

The radiation belts consist principally of electrons of up to a few MeV energy and protons of up to several hundred MeV energy. Energetic particles, which in the context of space systems radiation effects, can penetrate outer surfaces of spacecraft, for electrons, this is typically above 100 keV (0.1 MeV), while for protons and other ions this is above 1 MeV, [ECSS-E-10-04A].

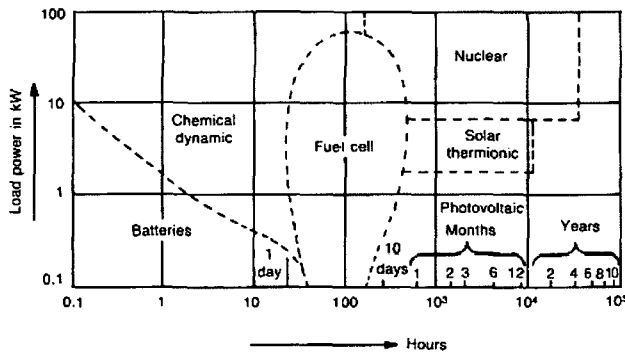


Fig. 1 Most suitable Satellite EPS components as a function of mission duration^[3]

It should be noted that the conversion efficiency of relevance to system design is array efficiency, rather than cell efficiencies. Array efficiencies are significantly lower than cell efficiencies mainly because the former reports minimum guaranteed array efficiencies under factory conditions. Whereas, the latter reports record (maximum) values under laboratory conditions.

GaAs solar arrays compared to Si solar arrays offer a good combination of high efficiency and high radiation resistance; the two, most important merits for space solar cells. Another type of solar cell material under research is indium phosphide (InP), which is similar to GaAs in efficiency, but is more resistant to radiation degradation. InP could be a good power supply for long duration applications such as on a Moon base.

Cascaded solar cell technologies include mechanically stacked cells, and monolithically cascaded cells. In the latter category, GaAs/Ge cells and InP/Si cells may be mentioned. In our proposal, the uni-junction GaAs/Ge solar arrays are used due to their high efficiency and radiation resistance. Figure 2 presents trends in space solar cell development. Figure 3 shows the I-V characteristics of GaAs/Ge solar cells.

2.2 Storage Battery Type Estimation

Storage battery provides the OBE with electrical power during satellite orbital flight (shadow segment and when power consumption of the load exceeds the power generated from SA) and also during ground satellite tests.

The satellite loads and the mission eclipse profile define the requirements for the battery design. The battery must

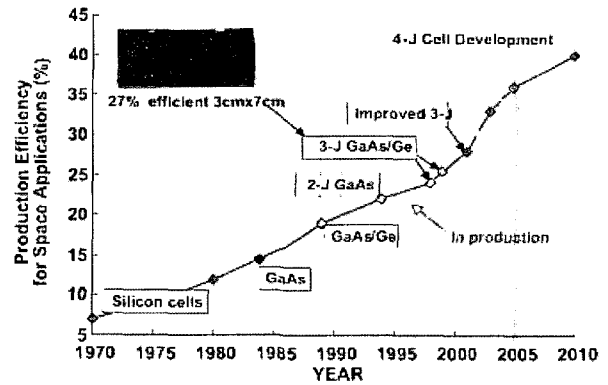


Fig. 2 Trends in space solar cell Development^[4]

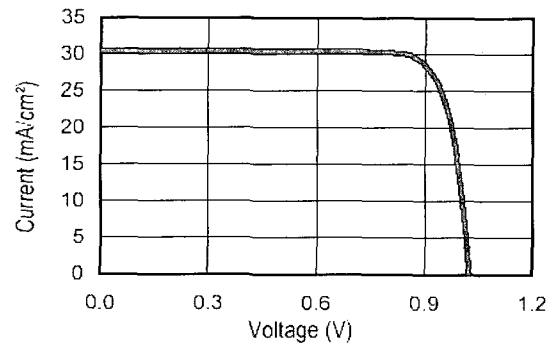


Fig. 3 GaAs/Ge Solar Cells I-V curve at AM0 (1353W/m²), 28°C^[5]

provide a low-impedance bus voltage in the specified range of 28.0±6.0V to power the OBE during an eclipse and to handle any loads that exceed solar array capability. The battery size is driven by resultant power demand, the duration of the power discharge and the total number of discharge cycles required by the mission. The battery must be tolerant of failure from a single cell in either open or short-circuit conditions. The battery design is also driven by restrictions such as operating temperatures and temperature gradients. The selection of battery technology was reduced to two candidate chemistries, NiH₂ cell technology and NiCd technology. Table 2 compares the main characteristics of both NiCd and NiH₂ batteries^[6].

The NiCd battery was chosen because of its safety record and because of its past success as a secondary power source. The charge and discharge characteristics of NiCd are illustrated in Figure 4 (a & b). The discharge curve is fairly consistent through most of its discharge

cycle and it can be recharged at 0.5C to virtually full capacity within the time allowed.

Table 2 Summary of NiCd and NiH₂ battery parameters

Battery_type Parameter	NiCd	NiH ₂
Energy density	30-40 WH/kg At battery level	35-50 WH/kg At battery level
Mass	Larger	Smaller
Volume	Smaller	Larger
Round efficiency.	≈ 80%	≈ 80%
Range of temp.	-5 to +50°C	-5 to +50°C
No of cycles	2-8*10 ³	2-7*10 ³

NiCd: It has the following advantages;

- Dependable and widely used technology for space missions.
- Provides high current with a rapid recharge capability.
- High tolerance to overcharging and is capable of over 6000 recharge cycles at 100% DOD, and
- Relatively low cost.

While it has two disadvantages;

- Prone to memory effect and Low cell voltage.

NiH₂: It is characterized by the following;

- It has more capacity than NiCd leading to fewer recharge cycles and No memory effect.
- While it has the following disadvantages;
- More heat generated during recharge than NiCd's.
- Requires complex charging to prevent damage from overheating and overcharge.
- Longer recharge times than NiCd.

Although the capacity of NiCd batteries may exhibit loss due to “memory effects,” or more accurately voltage depression, the degree to which this occurs can be minimized by varying the batteries’ depth of discharge (DOD) during their life cycle. Depending on the duty cycle of some power intensive subsystems such as communications, more power will be drawn on some orbits than on others. This will provide the battery with a varying DOD and should result in acceptable capacity during the satellite’s lifetime.

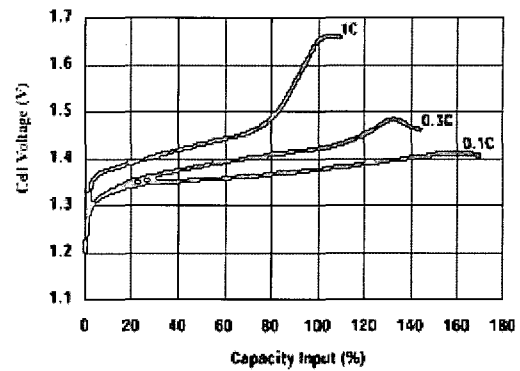


Fig. 4(a) Typical NiCd Battery charging Curves at 23°C

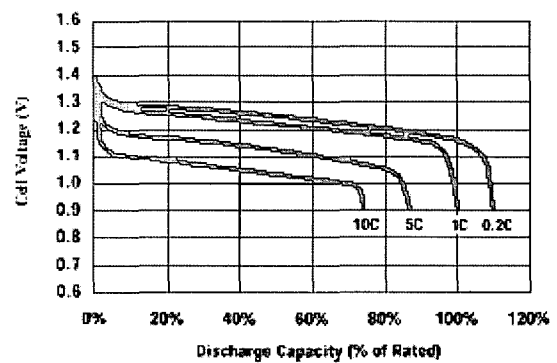


Fig. 4(b) Typical NiCd Battery discharging Curves at 23°C

Note: C is the nominal capacity of the storage battery.

3. Orbit selection

The orbit selection is strictly dictated by the requirements of the remote sensing payload. It must be ensured that the chosen orbit is technically feasible, bearing in mind the availability of various launch vehicles. It is convenient to divide the selection of a suitable orbit into two steps. Since the remote sensing user is invariably interested in comparing data from spatially distinct regions it is important that all data are collected from the same satellite altitude, so that all features on the ground appears on the same scale. This is achieved with a circular orbit around the Earth. Low Earth orbit is the generic term given to circular orbits with an altitude between 300 and 1500km. Such orbits predominantly use manned spacecraft and remote sensing satellites. Being much closer to the Earth greatly enhances spatial and radiometric resolutions. To avoid the risk of premature

orbit decay and to limit, as much as possible, significant orbit decay, the satellite should be placed in an orbit of at least 600km^[7].

The proposed satellite is Sun-synchronous with local time of passing the ascending node 10 hours and 30 minutes. The altitude of the circular orbit is ~ 670km, inclination ~98°, period of satellite orbit ~100min, approximately like the orbit of the satellite in^[1].

For orbits of such type, there are small variations in the orbit illuminations of the Sun and the Earth's shadow sections in revolutions during the whole flight's active lifetime. In the following sections an analysis of the orbit illumination pattern as well as solar array output power is introduced.

4. EPS Configuration and Block Diagram

The EPS includes solar arrays, storage batteries and a management and control device that estimates the appropriate mode of system operation. The control device controls signals and sends/receives the control commands and TM data exchanges.

The two major approaches for satellite EPS configuration design are; direct energy transfer (DET) and maximum power point tracking (MPPT)^[8]. In the DET method, the payload, subsystems and batteries are directly connected to the solar arrays and the extra power (at low temperatures and/or Beginning Of Life (BOL)) are absorbed (consumed) by shunt regulators while in the MPPT additional mechanisms and control devices are needed to track the Sun during operation. Because of the reliability parameters and complexity, the first proposal (DET) is applied.

The management and controller unit must control the excess solar array power that is not used for the loads or for battery recharge. It must monitor and maintain the health of the battery by optimizing the battery charge rate during battery refill after all battery discharges. It must prevent damage to the battery and satellite loads by protecting against an over-voltage or under-voltage condition of the power bus. Finally, it must interface with the satellite C&DH subsystem, provide EPS telemetry and receive ground commands^[6,9].

The management and controller unit controls the

charge/discharge process of the storage battery by controlling the output power from the solar array and protects the battery from fully discharging in the undesired or overloading sessions. Figure 5 shows the EPS block diagram based on the DET configuration.

The size of solar array could be estimated with the help of the value of the OBE loading (average power budget) and the specific output power of the solar array. Also the size of the storage battery capacity depends on the required amount of OBE energy during shadowing and eclipse periods.

5. Estimation of the specific output power from SA of the EPS

The specific output power from the EPS solar array (SA) depends on the type of SA, air mass zero (AM0 - 1360 W/m², 25°C) parameters, orbit parameters type, altitude and inclination of the orbit. The orientation of the solar arrays strongly affects the generated output power. From the energy balance point of view, the amount of average power that must be produced by the solar arrays, P_{sa} could be expressed as^[3,10-11]:

$$P_{sa} = \{(P_e * T_e / X_e) + (P_d * T_d / X_d)\} / T_d \quad (1)$$

Where:

- P_e and P_d are the power requirements during eclipse and daylight (power budget),
- X_e and X_d are the efficiency of the paths from the arrays to the batteries and the loads,
- T_e and T_d are the times in eclipse and daylight.

The specific output power from solar arrays at the terminals of the OBE could be expressed as follows:

$$P_{SA} (W / m^2) = P_n * FF * K_{ill} * K_{th} * K_{mppd} * \eta_{sys} * K_d \quad (2)$$

Where:

- P_n is the output power at begins of life;
- $P_n = AM0 (1358 W/m^2) * \eta_{SA} (\sim 0.2)$,
- FF is the filling factor of the solar array module; ~ 0.85,

- K_{ill} is the solar array surface illumination coefficient,
- K_{th} is the thermal coefficient of solar array,
- K_{mppd} is the matching factor between SA MPP and OBE loading, $\sim (0.9-1.0)$,
- η_{sys} is the energy transmission efficiency; ~ 0.87 ,
- K_d is the GaAs solar array degradation parameter; ~ 0.9

By estimating the specific output power from solar arrays and substitution to the get the results of P_{sa} , the required area of solar arrays can be estimated.

6. Estimation of the illumination and thermal coefficients

The illumination and thermal parameters depend on the satellite orbit analysis during the lifetime of the satellite. In the following, an analysis is done on orbit/attitude dynamics.

6.1 Coordinate Systems

Through the development of a mathematical model the following orthogonal coordinate system is used :

- Inertial Coordinate System (ICS) ($O_e X_i Y_i Z_i$) : the O_e origin coincides with the Earth center; axis $O_e Y_i$ is directed along the Earth axis of rotation; axis $O_e Z_i$ is directed to the vernal equinox; axis $O_e X_i$ completes the right hand side and lies on the equatorial plane.
- Sun Ecliptic Coordinate System (SECS) ($O_e X_s Y_s Z_s$) :

the $O_e Z_s$ axis is directed along the Earth-Sun vector; the $O_e Y_s$ axis is along the normal to the ecliptic; the $O_e X_s$ axis completes the right hand side and is directed towards the Sun's motion along the ecliptic.

- Orbital Coordinate System (OCS) ($O_b X_o Y_o Z_o$) : the O_b origin coincides with the spacecraft (SC) COM; the $O_b Z_o$ axis is directed along the radius vector that connects the center of Earth to the SC COM; the $O_b X_o$ axis is in the direction of flight.
- Design Coordinate System (DCS) ($O_d X_d Y_d Z_d$) : the O_d origin is in the SC-LV interface plane; axis $O_d Z_d$ is perpendicular to the spacecraft's launch vehicle (SC-LV) interface plane and is directed towards the LV; the $O_d X_d$ and $O_d Y_d$ axes lie in the plane of mating.
- Body Axes System (BAS) ($O_b X_b Y_b Z_b$) : the body axes are parallel and co directional to the DCS axes; in the case of an ideally oriented satellite, the body axes coincide with the OCS axes.

Figure 6 shows the satellite layout, orientation of solar arrays with respect to the Sun (angle α) and the body and design coordinate system, While Figure 7 shows the orientation of body with respect to orbit coordinate systems as a sequence of rotation (θ , ϕ , and ψ).

6.2 Orbit Dynamics

The orbit dynamics describe the translation motion (position and velocity) of a body (satellite or planet) orbiting another body. The satellite orbit and Sun orbit is propagated by the orbit generator given in Vallado^[12].

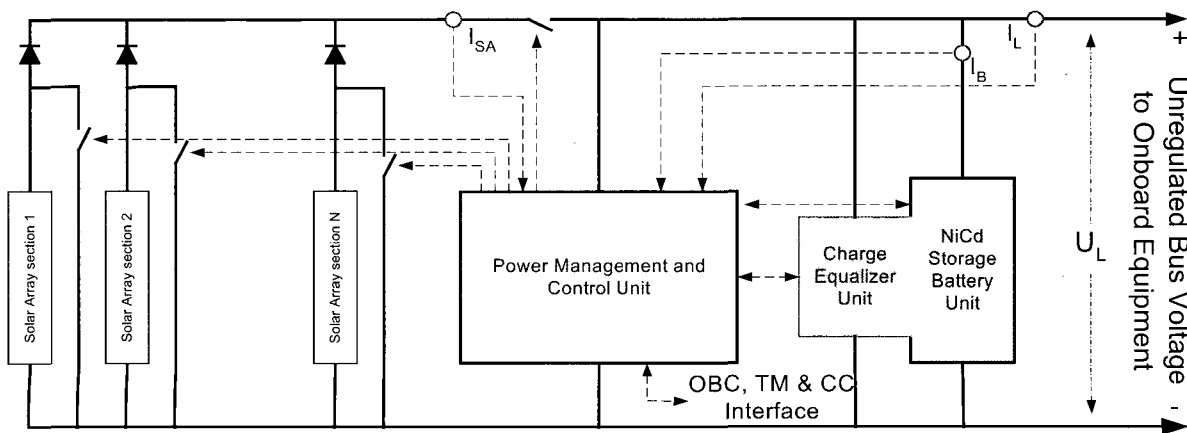


Fig. 5 Proposed microsatellite EPS block diagram

$$\ddot{\vec{r}} = -\frac{\mu}{r^3}\vec{r} + \vec{a}_p \quad (3)$$

Where:

\vec{a}_p is the vector of accelerations due to disturbances (gravity, aerodynamics solar radiation ...etc),
 \vec{r} is the position vector of the satellite in an inertial coordinate system. In modeling, two forces will be taken into account, gravitational force and aerodynamic drag.

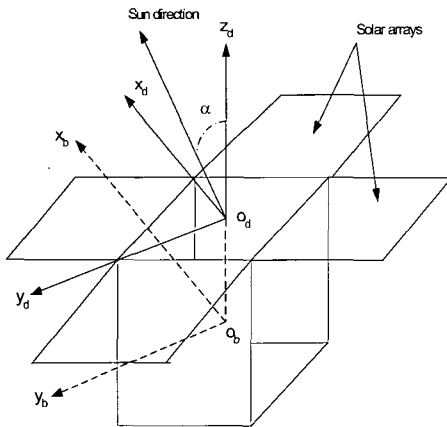


Fig. 6 Satellite layout

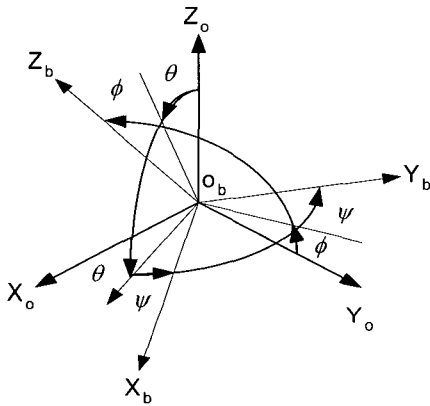


Fig. 7 Coordinate systems

6.3 Attitude Dynamics and Kinematics

Attitude is used to describe the orientation of one reference coordinate to another reference coordinate, such as a satellite body coordinate with respect to an inertial coordinates. Dynamic equations of motion on the BAS are as follow^[13,14]:

$$\omega_{bi}^{*b} = (J^b)^{-1} \cdot \left(\overline{M}_s^b + \overline{M}_{ctrl}^b - \omega_{bi}^b \times (J^b \cdot \omega_{bi}^b + H^b) \right) \quad (4)$$

Where:

- J^b is the satellite inertia,
- \overline{M}_s^b is the sum vector of disturbance moments,
- \overline{M}_{ctrl}^b is vector of control moment,
- $\omega_{bi}^b, \omega_{bi}^{*b}$ are SC absolute angular velocity and acceleration respectively,
- H^b is the angular momentum of the wheel.

The SC kinematics equation of motion around the COM in Quaternion form will be:

$$\dot{Q} = \frac{1}{2} \cdot Q \cdot \omega_{bo}^b \quad (5)$$

Where:

- $\dot{Q} = \dot{q}_0 + \dot{q}_1 + \dot{q}_2 + \dot{q}_3$ is the derivative of the Quaternion vector Q,
- ω_{bo}^b SC angular velocity relative to the OCS projected on the BAS.

For a Sun-synchronous LEO with a ~ 670 km altitude and a ~ 98 orbital inclination a software program was developed in the MATLAB. This program simulated changes in angle to a normal solar array plan with consideration of Sun direction, eclipse time and local time of ascension. The illumination coefficient is calculated with consideration of the orbital perturbations and accuracy of satellite separation from the launch vehicle. A sample of the developed program results is illustrated in Figure 8. The results show; the angle between the normal to orbit plan and Sun direction (Nue) in degree, the orbit Earth shadowing (TS) in min, current of SAs, Load and battery capacity (I_{SA}, I_L & Q_{SB}) as well as storage battery (SB) voltage and temperature (V_{SB} & T_{SB}). The results are illustrated in Figure 8.

The range of illumination parameters is found as (0.2438 min – 0.295 max; average ~ 0.265).

Also by analyzing the thermal parameters of the solar

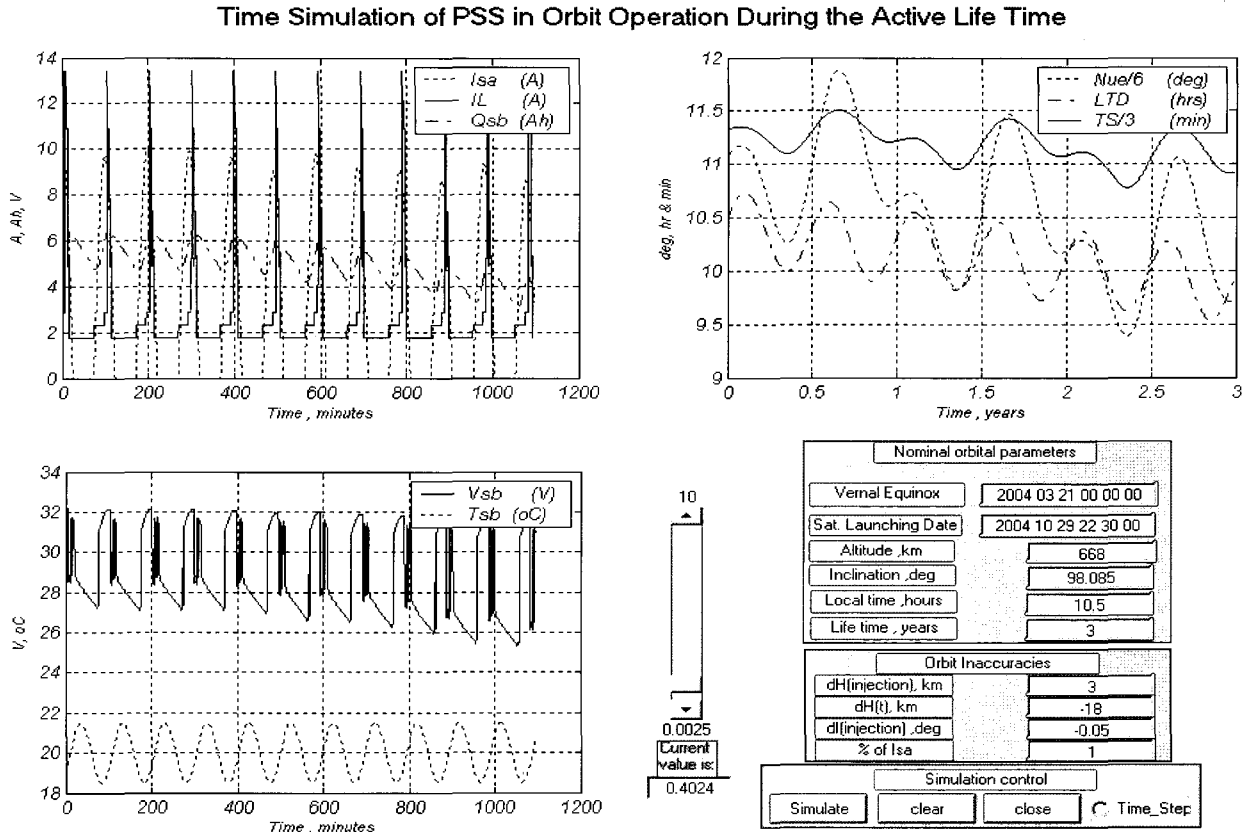


Fig. 8 A sample of the developed program results

array, it is found that it is ~ 0.9025 for GaAs solar arrays for the specified orbital altitude. So, the specific output power from the GaAs solar array could be estimated as follows:

$$\begin{aligned} P_{SA} (W / m^2)_{GaAs-BOL-max} &= K_{system} * K_d * K_{ill-max} \\ &= 54.4 W / m^2 \end{aligned} \quad (6)$$

$$\begin{aligned} P_{SA} (W / m^2)_{GaAs-EOL-min} &= K_{system} * K_d * K_{ill-min} \\ &= 39.8 W / m^2 \end{aligned} \quad (7)$$

The maximum output power is at the beginning of life and the best illumination coefficient is estimated as 87W while the power at the end of life and during the worst illumination is found as 63.5W. The average output power from the solar array at BOL can be estimated as follows:

$$\begin{aligned} P_{SA} (W / m^2)_{GaAs-BOL-av} &= K_{system} * A_{sa} * K_{ill-av} \\ &= 76.9 W \end{aligned} \quad (8)$$

7. EPS capability during detumbling mode

To estimate the capability of the EPS during detumbling mode, the disturbance and control moments of the microsatellite should be studied.

7.1 Disturbances and Control Moments

Satellites in orbit encounter small moments of disturbance from various environmental sources. These moments are either secular, which accumulate over time, or cyclic, which vary sinusoidally over an orbit. Both types are described by [13, 14].

Different environmental moments are more prevalent at different altitudes. In low Earth orbits (LEO) the largest environmental moments are gravity-gradient, magnetic,

and aerodynamic. In this paper, gravity-gradient, magnetic, solar radiation and aerodynamic moments are considered.

Usually, in detumbling mode, magnetorquers are used for control. It controls movement through the interaction of its magnetic field with terrestrial magnetic fields^[14].

7.2 Numerical Example

To demonstrate the effective power generated from the solar arrays during detumbling mode the following numerical example has been performed.

The Sun-synchronous low Earth orbit (LEO), mentioned above, is considered in this simulation. The satellite is assumed to have moment of inertia:

$$J = \begin{bmatrix} 16 & 0 & 0 \\ 0 & 16.7 & 0 \\ 0 & 0 & 14 \end{bmatrix} \text{ kg.m}^2$$

MATLAB software package used to integrate (simulate) the system of equations (3, 4, 5) and the angle α (angle between the Sun and normal to solar arrays is shown in Fig. 6) is determined.

Figure 9 shows the variation in angle α 500 minutes after separation from the LV. It is noted that during the

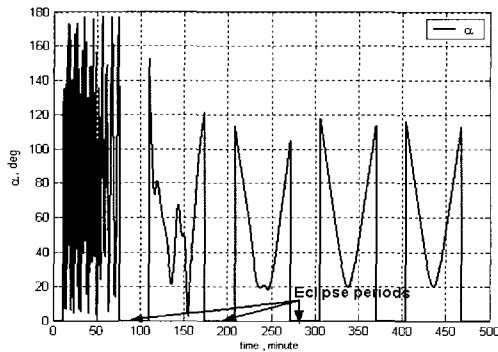


Fig. 9 Angle between the Sun and normal to solar arrays (Case1)

first 100 minutes, this angle changed quickly, as expected (because the satellite separates from the LV with a high angular velocity). However, after the angular velocity was suppressed, the variation became uniform, which was apparent in the last 200 minutes.

Three different cases were studied each case related to different initial conditions of attitude (angles and angular velocities at separation point). Table 3 shows the value of the illumination coefficient (average cosine of the angle α) that indicates the specific power generated from the solar arrays, as this coefficient increases the specific power increases.

8. Calculation of the available energy from EPS during detumbling mode

Table 4 shows a calculation of the available energy during detumbling and for two other successive steady state modes. It is noted that the EPS has a positive energy balance in all cases of the SB capacities. Hence the involved satellite OBE is capable of operating during detumbling mode without any off-nominal situations.

9. Conclusion

A power subsystem and its component characteristics are estimated and studied. The sizing of an Earth remote sensing microsatellite power supply is presented with a direct energy transfer configuration. GaAs solar cells and NiCd batteries are used to build the EPS for the microsatellite. Orbit dynamics, attitude dynamics and kinematics are analysed by developing a MATLAB based software program. The program takes into consideration orbit and solar array illumination patterns during the active lifetime of the satellite in orbit operation. Orbit perturbations and injection inaccuracies are also considered. The range of the solar array coefficients are

Table 3 Average Illumination coefficient ($\sum \cos(\alpha) / 100$ min period of time)

Time, minutes	0-100	100-200	200-300	300-400	400-500
Case 1	0.1844	0.3003	0.3455	0.2957	0.2982
Case 2	0.1879	0.2768	0.2957	0.2986	0.2967
Case 3	0.1663	0.3923	0.2906	0.2960	0.2975

Table 4 Available energy of EPS during detumbling mode.

Case	Period min	Kill	Power	Kill	Power	Kill	Power	Kill	Power	Kill	Power	
		0-100	100	100-200	200	200-300	300	300-400	400	400-500	500	
1		0.1844	48.10	0.3003	78.33	0.3455	90.10	0.2957	77.10	0.2982	77.80	
2		0.1879	49.00	0.2768	72.18	0.2957	77.13	0.2986	77.90	0.2967	77.37	
3		0.1663	43.40	0.3923	102.3	0.2906	75.78	0.2960	77.20	0.2975	77.60	
<i>Average power (W)</i>		46.8		84.27		81.0		77.4		77.6		
<i>Average available energy from the SA (Wh)</i>		78.0		140.5		135		129		129.3		
<i>Total available energy from PSS at 8Ah</i>		564.7 Wh					<i>The needed amount of energy for the satellite OBE during detumbling mode (300min) can be expressed as:</i> $P_{Sat} = \{ ADCS(40W \text{ max}) + PCDHS(41.5W \text{ max}) + PSS(4W) + GPS(4.2W \text{ max}) + CS_S - Band(3Wav) \}$ * 5hrs $P_{Sat} = 463.5Wh \text{ max}$					
<i>DOD at needed amount of energy %</i>		52.08%										
<i>Total available energy from PSS at 7Ah</i>		538.3 Wh										
<i>DOD at needed amount of energy %</i>		59.52%										
<i>Total available energy from PSS at 6Ah</i>		511.9 Wh										
<i>DOD at needed amount of energy %</i>		69.44%										

found between (0.2438 – 0.296) for a fixed solar array in a single path in the orbital coordinate system. Hence, the maximum and minimum specific SA power outputs are estimated in a range (39.8 – 54.4 W/m²) which takes into consideration the degradation of the SA and its best and worst illumination conditions.

An algorithm for simulating and controlling the satellite's attitude/orbit has been developed in order to determine the orientation of the solar arrays with respect to the sun direction during nominal and detumbling modes of operation. The angle between the sun and normal to the solar arrays is computed and an estimation of the output power from the solar arrays is calculated. A numerical example based on a LEO sunsynchronous remote sensing satellite demonstrates the efficiency of the solar arrays during the detumbling mode of operation.

The different conditions of the SB state of charge are considered and the EPS's available energy is estimated in each case. The energy balance results between the

available EPS and the needed OBE amount of energy confirm that the EPS is capable of providing the involved satellite subsystems with required energy during detumbling mode and nominal modes of operation without any off-nominal situations.

References

- [1] TERMA A/S Space Division, "Power Management and distribution Systems", www.terma.com.
- [2] D.G. Belov, et.al, "Electric Power Supply for Ocean Satellite", sixth European Space Power Conference, Porto, Portugal, 6-10 May 2002 (ESA SP -502, May 2002).
- [3] Wertz, J. and Larson, W., Eds., Space Mission Analysis and Design. Boston, Kluwer Academic Publishers, 1991.
- [4] ManTech for Multi-Junction Solar Cells, <http://www.afrl.af.mil/techconn/index.htm>.
- [5] Spectrolab Inc. 12500 Gladstone Avenue, Sylmar, California 91342 USA, www.spectrolab.com.
- [6] Paul E. Panneton and Jason E. Jenkins, "The MSX

Spacecraft Power Subsystem”, Johns Hopkins APL Technical Digest, Volume 17, Number 1 (1996).

- [7] S.R. Cvetkovic and G.J. Robertson, “Spacecraft Design Considerations for Small Satellite Remote Sensing”, IEEE Transaction on Aerospace and Electronic Systems, Vol. 29, No. 2, April 1993.
- [8] Masoum, Mohamed A.S. and Dehbonei, Hooman, “Design, Construction and Testing of a Voltage-based Maximum Power Point Tracker (VMPPT) for Small Satellite Power Supply”, 13th Annual AIAA/USU Conference on Small Satellites, SSC99-XII-7.
- [9] Andy Bradford, Luis M Gomes, Prof. Sir Martin Sweeting and Gokhan Yuksel, Cem Ozkaptan, Unsal Orlu, “ BILSAT-1: A Low-Cost, AGILE, Earth Observation Microsatellite for TURKEY”, 53rd International Astronautical Congress October 2002/Houston, Texas.
- [10] Greg Merritt and John Opiela, "Satellite Power Systems Sizing", www.tsgs.utexas/tadp/1995/spects/power.
- [11] You zheng , Gong ke, “Tsinghua Micro/Nanosatellite research and it's application”, 13th Annual AIAA/USU Conference on Small Satellites, SSC99-IX-3.
- [12] D. A. Vallado, *Fundamentals of Astrodynamics and Applications*. NY: McGraw-Hill, 1997.
- [13] Peter C. Hughes. *Spacecraft Attitude Dynamics*. John Wiley and Sons, New York, 1986.
- [14] James R. Wertz, editor. *Spacecraft Attitude Determination and Control*. Kluwer Academic Publishers, Dordrecht, 2000.



DR. IVANOVA Galina (Antonovna). Was born in Zaporozhye, Ukraine. Received her bachelor's degree in Physics & Engineering from the Dniepropetrovsk State University in Automatic Control Systems and completed her Ph.D at the Moscow Institute of Applied Mathematics in engineering mechanics theory. Currently is employed by Yuzhnoye State Design Office in the Satellite Attitude System Department.



Dr. Mohamed Bayoumy A. Zahran (M.Zahran), was born in Egypt, Received his B.Sc from Kima High Institute of Technology, M.Sc at 1993 and Ph.D. at 1999 from Cairo Univ, Faculty of Engineering, Electrical Power and Machines Dept. He is Researcher in the Electronics Research Institute, Photovoltaic Cells Dept. His experience in the field of renewable energy sources, systems design, management and control. Currently is employed by National Authority for Remote Sensing and Space Science in the Satellite EPS.



Eng. Mohamed Okasha (M.Okasha) was born in Egypt. Received his bachelor's degree from Cairo University Aerospace department. Currently is employed by National Authority for Remote Sensing and Space Science in the Satellite Attitude System Department, Cairo Egypt, e-mail: okasha77@hotmail.com